Front. Phys. China (2007) 1: 76−80
DOI 10.1007/s11467-007-0008-5

RESEARCH ARTICLE

LI Yan-li, YAO Kai-lun, LIU Zu-li

First-principle studies on the electronic structure of Fe_3O_4(110) surface

Abstract The first-principle was employed to study the six possible models for the Fe_3O_4(110) surface, namely the AB-terminated surface (AB model), the AB-terminated with Fe_A vacancy (AB-Fe_A vac model), the AB-terminated with Fe_B vacancy (AB-Fe_B vac model), the B-terminated surface (B model), the B-terminated surface with Fe_B vacancy (B-Fe_B vac model) and the B-terminated surface with O vacancy (B-O vac model). The stability, the electronic structure and the magnetic properties of the six surface models were also calculated. The results predict that the B-O vac model is more stable than other types of surface models. The half-metallic property remain in the AB and B models, while the other four surface models exhibit metallic properties. At the same time, the AB, AB-Fe_A vac, AB-Fe_B vac, B and the B-Fe_B vac models have ferrimagnetic properties, while the B-O vac model has antiferromagnetic property.

Keywords density functional theory, surface, electron density of states, magnetic properties

PACS numbers 71.15.Mb, 73.20.At, 74.25.Ha, 75.70.Rf

1 Introduction

In recent years, the surface structures and related physical properties of metal oxides have attracted more and more attentions for their potential applications. The thin films of the transition metal oxides have a wide range of technological applications in giant magneto-resistive (GMR) devices [1], catalysis [2] and spin valves [3] etc. Fe_3O_4 is a strongly correlated transition metal oxide, which is ferrimagnetic and the transition temperature is T_c = 851 K [4]. Bulk Fe_3O_4 has a cubic inverse-spinel structure at room temperature where the O^{2-} anions form an fcc lattice, one-third of the Fe ions (Fe^{3+}) occupy the tetrahedral interstices (A sites), and the other two-thirds of the Fe ions (half Fe^{3+} and half Fe^{2+}) are located in the octahedral interstices (B sites) [5−7]. The (110) surface layer of Fe_3O_4 can be described by two pairs of alternating atomic sublayers. Within a pair, one sublayer is composed of Fe_A (the A-site Fe cations), Fe_B (the B-site Fe cations) and O atoms, and the other sublayer is composed of Fe_B (the B-site Fe cations) and O atoms. The two sublayers are called AB-layer and B-layer, respectively. Based on the two structures of the sublayer, six models of the Fe_3O_4(110) surface will emerge immediately: (1) AB model: the surface is terminated with AB-layer. (2) AB-Fe_A vac model: the surface is the AB-layer with half of Fe_A vacancies. (3) AB-Fe_B vac model: the surface is the AB-layer with half of Fe_B vacancies. (4) B model: the surface is terminated with B-layer. (5) B-Fe_B vac model: the surface is the B-layer with half of Fe_B vacancies. (6) B-O vac model: the surface is the B-layer with one O atom vacancy per surface.

In this paper, we investigated the proposed six models of Fe_3O_4(110) surface in detail. Using first-principles method we calculated the stabilities and their electronic structures, respectively. Calculations show interesting results of atomic relaxations near surfaces, which provide new information on the low-index faces of Fe_3O_4.

LI Yan-li (✉), YAO Kai-lun, LIU Zu-li
Department of Physics, Huazhong University of Science and Technology, Wuhan 430074, China
E-mail: liyanli128@163.com

YAO Kai-lun
International Center of Materials Physics, Chinese Academy of Sciences, Shenyang 110015, China

Received October 16, 2006

2 Methodology

The calculations were performed in the framework of density functional theory (DFT) within the generalized gradient approximation (GGA96). We employed the full potential linearized augmented plane wave (FPLAPW) method as implemented in the Wien2k package [8] and the self-interaction corrected (SIC) LDA+U calculations with the electron

electron correlation, at the same time, the spin-orbit coupling was taken into account to supplement the generalized gradient approximation (GGA) results. In this LDA+U (SIC) method, the strong correlation between localized d-electrons is explicitly taken into account through the screened effective electron-electron interaction parameter $U_{\text{eff}} = U - J$ with U and J denoting the Coulomb and exchange integral, respectively. We used the value of $U = 0.50$ *Ry* (6.800 eV) and $J = 0.12$ *Ry* (1.632 eV), which is to say $U_{\text{eff}} = 0.38$ *Ry* (5.168 eV). The plane-wave cut off energy is 340 eV. In the atomic sphere regions, the basic set consists of spherical harmonics with azimuthal quantum number $l \leqslant 10$, and non-spherical contributions of the charge density and potential with $l \leqslant 5$, and the charge density was Fourier expanded up to $G_{\max} = 14$. For the Brillouin zone integration, we used 200 k-points in the whole first Brillouin zone (30 k points in the irreducible part of the surface Brillouin zone) [5]. This set of parameters assures a total energy convergence of 3.0×10^{-5} eV per atom. All the chosen parameters are consistent during the calculations.

3 Surface calculations

The Fe_3O_4 (110) surface is simulated by a symmetric surface supercell containing five AB and four to six B layers depending on the structure model [12]. The vacuum between the periodic slabs amounts to 10 Å. The outermost 2–4 layers are fully relaxed and the interlayer atoms are fixed.

By relaxation calculations, we find that the outermost surface atoms of the six Fe_3O_4 (110) surface models are always found to be O atoms, which can be seen in Table 2. This might be due to the fact that the outermost atoms allow O anions, which attract more valence electrons than the Fe cations, to spread out the electron clouds into the vacuum to reduce the kinetic energy and accordingly to lower the systems' energy [5]. The magnetic moments of the ideal and relaxed structures for the six surface models with respect to the bulk magnetic moments are listed in Table 1. The magnetic moments of the ideal surface structures are enhanced due to the surface effects, which for the relaxed surface structures, the magnetic moments of the AB, AB-Fe_B vac, and B models are reduced when the atomic relaxation is allowed to take place.

Table 1 The changes in magnetic moments (positive for increase and negative for decrease) of the five ferrimagnetic surface models in the ideal and relaxed structures compared to the bulk magnetic moments. The units are μ_B per surface area.

Models	AB	AB-Fe_A vac	AB-Fe_B vac	B	B-Fe_B vac
Ideal	+1.28	+1.12	+1.61	+2.3	+0.47
Relaxed	−0.36	+0.28	−0.36	−0.27	+0.24

In the AB model, the surface is terminated with Fe_A, Fe_B and O atoms. We have calculated the magnetic moment for Fe_A ($-3.37\,\mu_B$) and Fe_B ($3.58\,\mu_B$) in the bulk Fe_3O_4, which are in agreement with the experimental values $-3.50\,\mu_B$ [8] and $3.60\,\mu_B$ [9]. The magnetic moments of Fe_A and Fe_B in the outermost surface for the relaxed AB model are $-3.08\,\mu_B$ and $3.17\,\mu_B$, which are smaller than the corresponding values in the bulk Fe_3O_4. A more interesting result in the relaxation calculations is that the outmost AB-layer that is split into three layers with the O atoms being the outermost surface atoms, the two Fe_A atoms situate at the second sub-layer and the two Fe_B atoms situate at the third sub-layer. The distance of the outermost surface O atoms layers and the Fe_A atoms in the sub-layer is 0.18 Å. At the same time, the B-layer next to the surface AB-layer also split into three layers with two Fe_B atoms and two O atoms move outward, but the moving distance of the two Fe_B atoms is larger than the two O atoms and the other two O atoms almost have not moved. The optimized results of the distance between the layers are listed in Table 2.

Table 2 Optimized results of the interlayer relaxations for the six surface models in terms of absolute distance (Å), the values between ↑ and ↓ are the distance between the relaxed layers from the outermost surface to the interlayer.

AB	AB-Fe_A vac	AB-Fe_B vac	B	B-Fe_B vac	B-O vac
4O	**4O**	**2O**	**4O**	**O**	**O**
↑	↑	↑	↑	↑	↑
0.24	0.36	0.18	0.67	0.28	1.02
↓	↓	↓	↓	↓	↓
2Fe_A	**Fe_A**	**2O**	**2Fe_B**	**O**	**2Fe_B**
↑	↑	↑	↑	↑	↑
0.12	0.52	0.54	0.42	0.14	0.26
↓	↓	↓	↓	↓	↓
2Fe_B	**Fe_B (B-layer)**	**2Fe_A**	**2Fe_A**	**O**	**2O**
↑	↑	↑	↑	↑	↑
0.28	0.08	0.22	0.06	0.59	0.04
↓	↓	↓	↓	↓	↓
2Fe_B	**2Fe_B (AB-layer)**	**3Fe_B**	**2Fe_B**	**3Fe_B**	**2Fe_B**
↑	↑	↑	↑	↑	↑
0.30	0.17	0.54	0.31	0.34	0.25
↓	↓	↓	↓	↓	↓
2O	**Fe_B (B-layer)**	**2O**	**4O**	**2Fe_A**	**2O**
↑	↑	↑		↑	↑
0.67	0.43	0.34		0.15	0.04
↓	↓	↓		↓	↓
2O	**O**	**2O**		**3O**	**2 Fe_A**

In the AB-Fe_A vac model, the surface is the AB model with half monolayer of Fe_A. After full relaxation the outermost AB-Fe_A vac layer also split into three layers with the O atoms being the outermost surface atoms, which is similar to the AB model. The Fe_A atom situated at the second sub-layer and two Fe_B atoms of the first layer move underneath the Fe_B of the second layer. The distance of the outermost O atoms layers and the Fe_A atoms in the sub-layer is 0.21 Å. At the same time, the B-layer next to the surface AB-layer split into three layers with two Fe_B atoms and one O atom move outward, and the other three O still situate at the original position. The magnetic moments of Fe_A and Fe_B in the outermost surface layer are about $0.5\mu_B$ and $0.06\,\mu_B$ less than those in the bulk, which are $-3.37\,\mu_B$ and $3.58\,\mu_B$.

In the AB-Fe_B vac model, the surface is the AB model with a half monolayer of Fe_B. The results of the relaxations

are similar to the above two models. Both of the outermost surface layer and the second layer split into the three sub-layers. However, the difference is that the two Fe_B atoms of the second layer move into the same layer with the Fe_B atom of the first layer. The distance of the outermost surface O atom layers and the O atoms in the sub-layer is 0.12 Å, which is smaller than the other surface models. The magnetic moments of Fe_A and Fe_B in the outermost layer are reduced to $-2.87\ \mu_B$ and $3.52\ \mu_B$ compared to the value $-3.37\ \mu_B$ and $3.58\ \mu_B$ of bulk Fe_3O_4.

In the B model, the surface is terminated Fe_B and O atoms. The outermost surface layer splits into two sub-layers and the second layer is split into three sub-layers. The sequence is $4O–2Fe_B–2Fe_A–2Fe_B–4O$. The distance of the outermost O atom layers and the Fe_B atoms in the sub-layer is 0.53 Å.

In the B-Fe_B vac model, the surface is the B model with half monolayer of Fe_B. After relaxation we find that three O atoms of the outermost surface move outward while one O atom relaxes inward. The distance of the outermost surface O atom layers and the next O atom layer is 0.33 Å. At the same time, the Fe_B atoms of the first layer and the second layer move into the same layer. One O atom of the second layer moves inward the bulk and the other three O atoms still remain at the original position. The magnetic moment of Fe_A in the model is $-3.61\ \mu_B$, which is larger than $-3.37\ \mu_B$ of the bulk. The magnetic moment of Fe_B in the B-Fe_B vac model is $3.30\ \mu_B$, which is smaller than $3.58\ \mu_B$ of the bulk.

In the B-O vac model, the surface is the B model with one O atom vacancy per surface. The magnetic moment of the Fe_A and Fe_B in the outermost surface layer are $-3.16\ \mu_B$ and $3.28\ \mu_B$. At the same time, we find that one O atom of the first layer relaxes outward the vacuum and the other two O atoms move inward the bulk. The distance of the outermost surface O atom layers and the Fe_B atoms in the sub-layer is 0.89 Å, which is the largest of the six models. The sequence of the relaxed slab is $O–2Fe_B–2O–2Fe_B–4O–2Fe_A–2O$ and the interlayer distance of the relaxed surface structure is listed in Table 2.

We find that the relaxation effect plays an important role in the change of atom magnetic moments of Fe_3O_4 (110) surface by investigating the six surface models with relaxations.

To compare the relative stabilities of the six Fe_3O_4(110) surface models, we calculated the surface free energy σ of Fe_3O_4(110) surface according to the following formula [10]:

$$\sigma = (E_{\text{surface}} - N_{\text{Fe}}\mu_{\text{Fe}} - N_{\text{O}}\mu_{\text{O}})/2A \tag{1}$$

Here, E_{surface} is the total energy of the slab, which is the resulting DFT energy of the slab for 0 K. μ_{Fe} and μ_{O} are the chemical potentials of Fe and O in the slab, respectively. In addition, N_{Fe} and N_{O} are the numbers of the Fe and O atoms in the slab. A is the surface area of the Fe_3O_4(110) surface cell. The total chemical potential of the elemental Fe and O is in equilibrium with that of bulk Fe_3O_4: $\mu_{Fe_3O_4(\text{bulk})} = 3\mu_{\text{Fe}} + 4\mu_{\text{O}}$. Accordingly, Eq. (1) becomes

$$\sigma = \left[E_{\text{surface}} - \frac{1}{3}N_{\text{Fe}}\mu_{Fe_3O_4(\text{bulk})} + \left(\frac{4}{3}N_{\text{Fe}} - N_{\text{O}}\right)\mu_{\text{O}} \right]/(2A) \tag{2}$$

The surface free energy depends now only on the oxygen level. The upper and lower limits of μ_{O} are obtained by preventing the gas phase O from condensing on the sample and O atoms in the slab from leaving the sample, respectively. The lower boundary and the upper boundary for μ_{O} will be called the O-poor limit and the O-rich limit. Therefore, the range of the O chemical potential is [11, 12]:

$$\Delta H_{\text{f}}^0 \leqslant \mu_{\text{O}} - \mu_{\text{O}}^{\text{gas}} \leqslant 0 \tag{3}$$

where ΔH_{f} is the 0 K formation heat of bulk Fe_3O_4, which is taken to be −2.968 eV. The O chemical potential is referenced with respect to the total energy of an oxygen molecule. $\Delta\mu_{\text{O}} = \mu_{\text{O}} - \mu_{\text{O}}^{\text{gas}} = \mu_{\text{O}} - (1/2)E_{\text{O}_2}^{\text{total}}$. The surface free energy of the six Fe_3O_4 (110) surface models as a function of oxygen chemical potential according to Eq. (2) are given in Fig. 1.

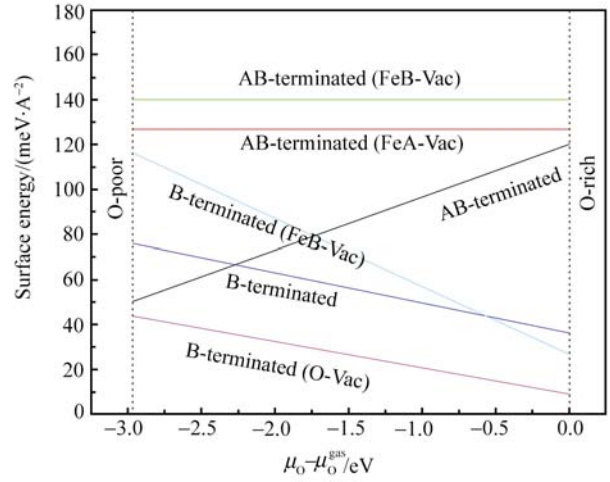

Fig. 1 Surface energies of Fe_3O_4(110) as a function of the chemical potential of oxygen for the six surface models.

First, the surface energies of the AB-Fe_A vac and AB-Fe_B vac models are independent of the chemical potential, while the surface energies of the AB, B, B-Fe_B vac and B-O vac models are linearly dependent on the oxygen chemical potential. With the increase of the oxygen chemical potential, the free energies of the B, B-Fe_B vac and B-O vac models decrease, while that of the AB model increases. As we all know, a surface with a large surface energy is in a rather unfavorable state. From Fig. 1, we can see that the B-O vac surface model has the lowest surface energy over the whole range. That is to say, the B-O vac surface model appears to be more stable than other surface models, which is the most probable surface structure among the supposed six surface models.

Second, the B, B-Fe_B vac and B-O vac surface models are

more stable than the AB, AB-Fe_A vac and AB-Fe_B vac surfaces at higher oxygen levels because they have relatively lower free energies. According to Fig. 1, the AB model is relatively more stable compared to the B and B-Fe_B vac models in an O-poor atmosphere. As the oxygen chemical otential $\mu_O - \mu_O^{gas}$ increases, the B and B-Fe_B vac surfaces gradually become stable. We also find that the AB-Fe_A vac and AB-Fe_B vac surfaces are less stable than the other surfaces over the whole allowable range for they have relatively larger free energies.

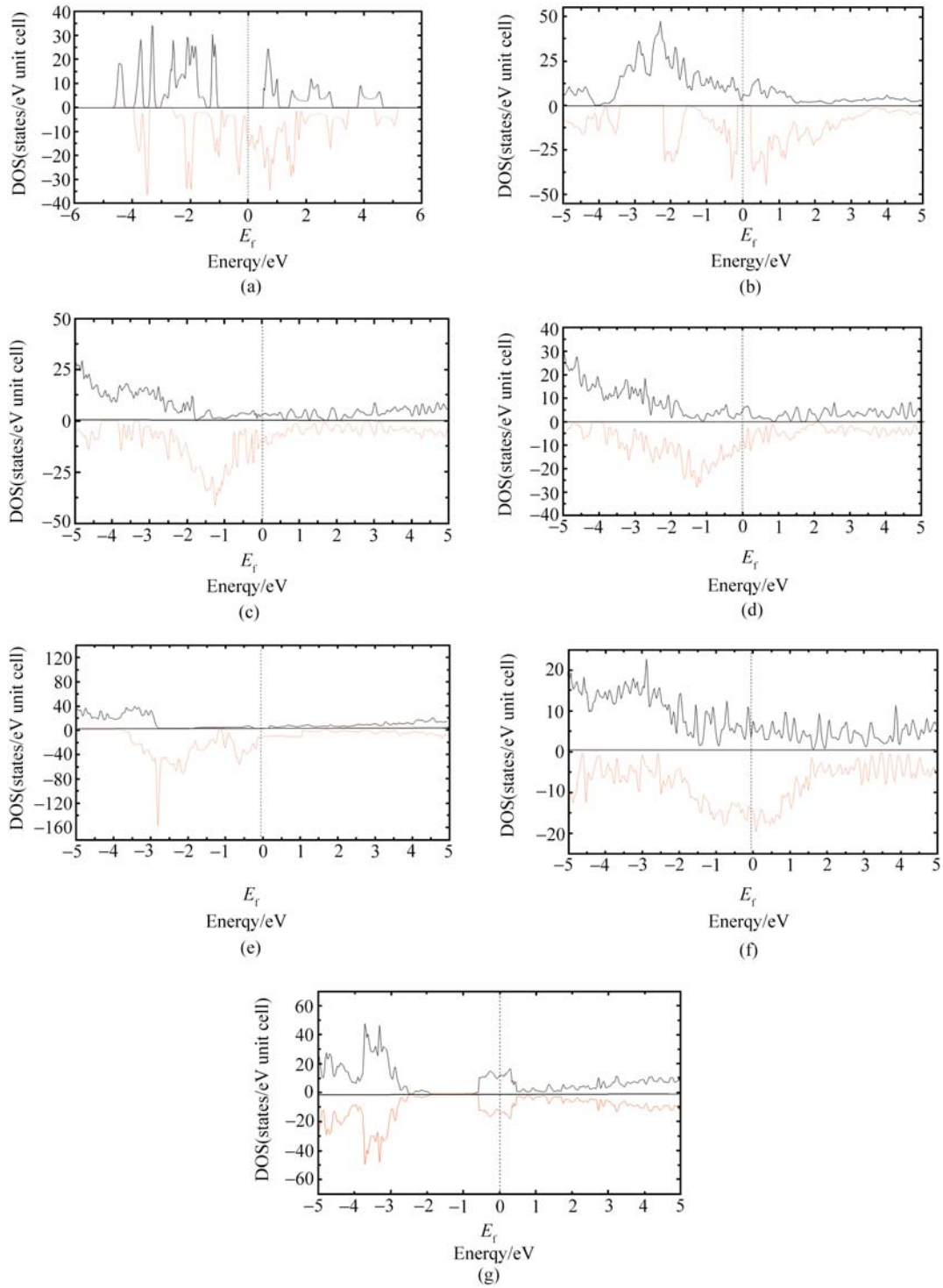

Fig. 2 Density of states for **(a)** the bulk Fe_3O_4; **(b)** the Fe_3O_4 (110)-AB Surface; **(c)** the Fe_3O_4 (110)-AB Fe_A vac Surface; **(d)** the Fe_3O_4 (110)-AB Fe_B vac surface; **(e)** the Fe_3O_4 (110)-B surface; **(f)** the Fe_3O_4(110)-B Fe_B vac surface; **(g)** the Fe_3O_4 (110)-B O vac surface. (*dark solid*: spin-up states; *red dashed*: spin-down states; *dotted*: the Fermi level)

4 Electronic structure calculations

In order to further investigate the magnetic properties of the six surface models for Fe_3O_4 (110) surface, we also give the total density of states (DOS) of the bulk Fe_3O_4 and the six proposed models for the Fe_3O_4 (110) surface in Fig. 2. As shown in Fig. 2, the plotted energy range is from −5 eV to 5 eV. Because the DOS distribution near the Fermi level determines the magnetic properties, we concentrate our attentions on the DOS in the vicinity of the Fermi level, which is set to zero. In the bulk, Fe_3O_4 shows a half-metallic behavior with a band gap in the majority-spin channel of approximately 0.5 eV and 100 % spin polarization due to the t_{2g} states of FeB at E_F in the majority-spin channel. On the other hand, we notice that in the vicinity of the Fermi level the total spin-up and the spin-down DOS are obviously split off for the AB, AB-Fe_A vac, AB-Fe_B vac, B and B-Fe_B vac surface models. At the same time, we find that there exist antiferromagnetic interactions between the atoms in the surface cells by calculation of the magnetic moment and the total magnetic moment of the surface cell is not equal to zero, which indicates that the above five possible surfaces all have ferrimagnetic properties. From Fig. 2 (g), we can see that the DOS of the spin-up and spin-down electrons have the same shape, which demonstrates that the B-O vac surface has antiferromagnetic properties.

On the other hand, we also find that for the AB model, the energy gap in the spin-down subbands is opened, and the spin-up total DOS is continuous in the vicinity of the Fermi level. The spin-up subbands exhibit metallic properties and the spin-down subbands insulator properties. The gap of the spin-down band is about 1.74 eV. The metal and insulator behaviors coexist in the AB-terminated surface, which shows that the half-metallic property remains in the AB model. In the B model, the spin-up subbands show insulator properties and the spin-down subbands show metallic properties. The gap of the spin-down band is about 0.76 eV. That is to say, the B-terminated surface is also a half-metallic magnet.

For the AB-Fe_A vac, AB-Fe_B vac, B-Fe_B vac and B-O vac models, both of the spin-up and the spin-down DOS cross the Fermi level, therefore the four surfaces have metallic properties, which are different from the properties of the bulk Fe_3O_4.

5 Summary and conclusions

Using the DFT theory, we investigated the six possible structures of Fe_3O_4 (110) surface. The stability, the electronic structure and the magnetic properties of the six surface models were also calculated. The results predict that the B-O vac surface model is the most stable structure among the six possible models. The AB and B models have half-metallic property, while the other four surface models exhibit metallic properties. From the DOS plot, it is found that the AB, AB-Fe_A vac, AB-Fe_B vac, B, and the B-Fe_B vac surface models have ferrimagnetic properties, and the B-O vac model has antiferromagnetic property, which are different from the properties in the bulk Fe_3O_4. To our best knowledge, it is the first time to predict the possible structure for Fe_3O_4 (110) surface in theory and lack of results in experiment. So we look forward to further experimental results.

Acknowledgements We acknowledged the support from the National Natural Science Foundation of China under the Grant Nos.10574048 and 20490210.

References

1. Wolf S. A., Awschalom D. D., Buhrman R. A., et al., Science, 2001, 294: 1488
2. Noguera C., Physics and Chemistry at Oxide Surfaces, Cambridge: Cambridge University Press, 1996
3. van Dijken S., Fain X., Watts S. M., and Coey J. M. D., Phys. Rev. B, 2004, 70: 052409
4. Dedkov Y. S., Fonin M., Vyalikh D. V., et al., Phys. Rev. B, 2004, 70: 073405
5. Cheng C., Phys. Rev. B, 2005, 71: 052401
6. Ahdjoudj J., Martinsky C., Miont C., et al., Surf. Sci., 1999, 443: 133
7. Rakhecha V. C. and Satya Murthy N. S., J. Phys. C, 1978, 11: 4389
8. Blaha P., Schwarz K., Madsen G. K. H., et al., University of Technology, 2002; Improved and updated Unix version of the original copyrighted Wiencode, which was published by Blaha P., Schwarz K., Sorantin P., and Trickey S. B., Comput. Phys. Commun., 1990, 59: 399
9. Fonin M., Pentcheva R., Dedkov S., et al., Phys. Rev. B, 2005, 72: 104436
10. Reuter K. and Scheffler M., Phys. Rev. B, 2001, 65: 035406
11. Liu L. M., Wang S. Q., and Ye H. Q., Acta Mater, 2004, 52: 3681
12. Pentcheva R., Wendler F., Meyerheim H. L., et al., Phys. Rev. Lett., 2005, 94: 126101